



THE UNIVERSITY *of* EDINBURGH

Edinburgh Research Explorer

## Withdrawal resistance of the self-tapping screws in engineered bamboo scrimber

**Citation for published version:**

Li, H, Qiu, H, Wang, Z & Lu, Y 2021, 'Withdrawal resistance of the self-tapping screws in engineered bamboo scrimber', *Construction and Building Materials*, vol. 311, 125315.  
<https://doi.org/10.1016/j.conbuildmat.2021.125315>

**Digital Object Identifier (DOI):**

[10.1016/j.conbuildmat.2021.125315](https://doi.org/10.1016/j.conbuildmat.2021.125315)

**Link:**

[Link to publication record in Edinburgh Research Explorer](#)

**Document Version:**

Peer reviewed version

**Published In:**

Construction and Building Materials

**General rights**

Copyright for the publications made accessible via the Edinburgh Research Explorer is retained by the author(s) and / or other copyright owners and it is a condition of accessing these publications that users recognise and abide by the legal requirements associated with these rights.

**Take down policy**

The University of Edinburgh has made every reasonable effort to ensure that Edinburgh Research Explorer content complies with UK legislation. If you believe that the public display of this file breaches copyright please contact [openaccess@ed.ac.uk](mailto:openaccess@ed.ac.uk) providing details, and we will remove access to the work immediately and investigate your claim.





24 the axis of the STS. It has also been found that a critical anchoring slenderness ratio is around  
25 7.5, and a longer embedment length would lead to the rupture of the STSs. For the calculation  
26 of the withdrawal resistance of the STSs in bamboo scrimber, several relevant calculation  
27 formulas are examined, and a modified formula is proposed. Verification of the modified  
28 formula against the current test results as well as relevant data from the literature shows  
29 satisfactory accuracy.

30 **Keywords:** Bamboo scrimber; Self-tapping screw; Anchor performance; Withdrawal  
31 resistance

## 32 **1 Introduction**

33 As a renewable material that can be used in structural engineering [1-3], engineered bamboo  
34 has attracted a lot of attention in the research community in recent years, with much of the  
35 interest focused on the mechanic behaviour and the processing technology [4-11]. While  
36 timber is more widely used in building structures, in many parts of the world such as China  
37 the timber resources are limited and the industrial use of timber relies heavily on imports. On  
38 the other hand, there exist numerous bamboo species and vast bamboo forest areas in many of  
39 those regions. From the structural application point of view, the tensile strength and  
40 compressive strength of bamboo are actually higher than wood, at about 2 times and 1.1 times  
41 that of wood, respectively [12]. The more recent advances in the processing technologies and  
42 industrialization level have promoted the production of engineered bamboo with excellent  
43 mechanical properties, such as glued bamboo [13], bamboo scrimber [14], laminated bamboo  
44 lumber [15] and bamboo-wood composite materials [16].

45 As one of the main engineering products in the market recently [17], bamboo scrimber is

46 made by gluing the bamboo filament bundles together. The bamboo culm is disassembled into  
47 long bamboo strands firstly. After being dried and charred, the strands can be put into the  
48 molds and pressed into parallel bamboo strand lumber under hot pressing (or cold pressing)  
49 [18]. Both the tensile and compressive strengths along the grain of bamboo scrimber are  
50 higher than those of the wood material made from larch and spruce, with relatively low  
51 variability in material properties [19]. The tensile strength and modulus of elasticity along the  
52 bamboo grain can reach 100MPa and 10GPa, respectively. Thus, the bamboo scrimber has  
53 been used not only widely in furniture [20, 21], but also in building and bridge structures [18,  
54 22]. The current research of bamboo scrimber generally focuses on the beam and column  
55 components [23-26]. However, the investigation on the connections in a bamboo scrimber  
56 structure is limited [27, 28]. In fact, the connection is often a weak link in a bamboo scrimber  
57 structure and so a sound connection design plays a key role in ensuring the integrity, strength  
58 and stiffness of the whole structure [28, 29]. Therefore, it is necessary to investigate the  
59 bamboo scrimber connection in detail.

60 The mechanical performance of the self-tapping screws (STSs) has improved with the  
61 progress of the metal processing technology. The STSs have shown potential in the beam-to-  
62 beam connection in timber structures [30-33]. Generally speaking, the STSs can reduce the  
63 possibility of splitting while used with small spacing and edge distance and increase  
64 operational efficiency. Besides, such a connection with STSs also possesses an aesthetical  
65 appearance and robust mechanical behavior [32]. Furthermore, STSs are effective in  
66 reinforcing timber joints [34], and they can also effectively transfer in-plane shear forces in  
67 connections of CLT shear walls and diaphragms [35]. Using fully threaded STS in the

68 bamboo scrimber connections is a possible efficient choice.

69 In the above regards, the withdrawal resistance of the STSs in bamboo scrimber becomes  
70 a key factor. However, the research on the withdrawal resistance of the STSs in bamboo  
71 scrimber is still limited [21, 36, 37]. Test results of screw joints in bamboo scrimber furniture  
72 have shown that the screw-in depth and hole diameter have a significant influence on the pull-  
73 out resistance, whereas the type of screws has no apparent effect [21, 36]. It has been found  
74 that the face and edge withdrawal resistances of screws in bamboo scrimber tend to be higher  
75 as compared with those in medium-density fiberboard and particleboard [37]. It is also  
76 generally understood that the withdrawal resistance in bamboo scrimber used in furniture and  
77 structural applications has similar relations with the pilot hole diameter [21, 37]. More  
78 specifically, the withdrawal resistance of screws embedded in *Phyllostachys edulis* bamboo  
79 culm walls has been investigated and compared by a modified ASTM D1761 test [38]. Li et al  
80 [39] suggested that a suitable diameter of the guiding hole should be 80%–90% of the  
81 diameter of the screw in laminated bamboo lumber. Zhang [40] found that the relationship  
82 between the withdrawal resistance and the embedding depth of screw in Glued Laminated  
83 Bamboo followed a linear function. However, there is a lack of information regarding the  
84 influence of the screw angle on the withdrawal resistance of the STSs in bamboo scrimber,  
85 and moreover the calculation of the withdrawal resistance has not been investigated.

86 This paper presents an experimental investigation into the withdrawal resistance of self-  
87 tapping screws (STSs) inserted in bamboo scrimber for structural applications, with three  
88 common screw diameters. The influences of the STS embedment length, screw diameter and  
89 screw angle on the failure mode and the withdrawal resistance are investigated systematically.

90 Furthermore, several relevant calculation formulas are applied to estimate the withdrawal  
91 resistance of STS in bamboo scrimber. These include formulas in Eurocode 5 [41] and  
92 CCMC13677-R [42], which are originally suited for the screw bearing capacity in timber, and  
93 an empirical formula [43] for the withdrawal resistance in the raw bamboo. The results are  
94 compared and analysed. On this basis, modified formulas for the calculation of the  
95 withdrawal resistance of the STSs at an angle of 0° and 90° with the bamboo scrimber fiber  
96 are proposed.

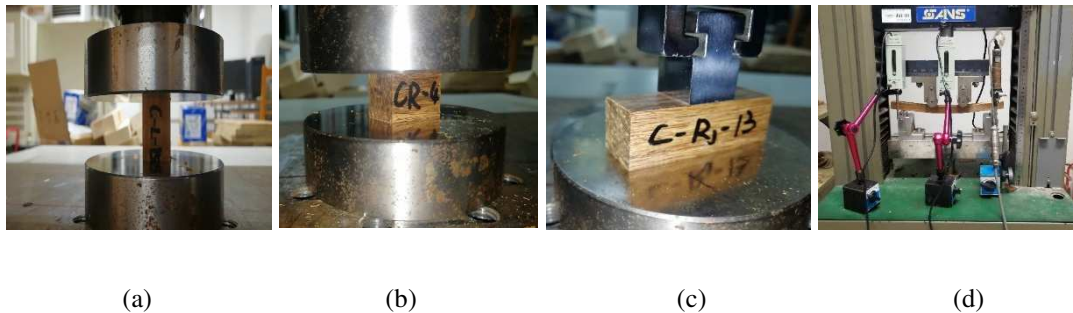
## 97 **2. Experimental program**

### 98 2.1 Materials

99 The materials involved in this study include bamboo scrimber and STSs. The bamboo  
100 scrimber was supplied by a bamboo material producer in Jiangxi province, China. According  
101 to the "testing methods for physical and mechanical properties of bamboo used in building"  
102 [44], the average moisture content of the bamboo scrimber was determined to be 9.8%, and  
103 the average air-dry density was 1.05 g/cm<sup>3</sup>. A total of 75 compressive tests and 6 bending  
104 tests of bamboo scrimber material were performed (Fig.1). The cross-sections of the samples  
105 were uniformly 20 mm × 20 mm. For compression tests, the sample specimens were 30 mm  
106 in length and the compressive loads were applied at the two ends of the samples via rigid steel  
107 plates [45, 46]. For the bending tests, specimens were 300mm in length and the tests were  
108 performed according to the ISO 3349 standard [47]. The compressive tests and bending tests  
109 of the samples were carried out using a 100kN mechanical testing machine and a 30 kN  
110 mechanical testing machine, respectively. Both types of tests were performed under a  
111 displacement control mode, and the loading rate was 5mm/min for the compression tests and  
112 4mm/min for the bending tests.

113 The test results for the properties of the bamboo scrimber are shown in Table 1. It can  
114 be observed that the relative difference of the total compressive strength in the radial and

115 tangential directions of the bamboo scrimber is only 2.9%. The relative difference of the local  
 116 compressive strength in these two directions is also small, at 7.8%. This may be explained by  
 117 the fact that in the process of restructuring bamboo, all four sides are compressed and the  
 118 bamboo filaments are tightly combined, and as a result the mechanical properties of the two  
 119 horizontal grain directions are close to each other. According to a separate experiment on the  
 120 same bamboo scrimber [48], the compressive modulus of elasticity in the direction parallel to  
 121 the grain is 11890 MPa, and that perpendicular to the grain is 1365 MPa.



124 **Fig. 1.** Test of material properties of bamboo scrimber: (a) Compressive strength parallel to the grain,  
 125 (b) compressive strength perpendicular to the grain, (c) Local compressive strength perpendicular to  
 126 the grain, and (d) Bending strength

127 **Table 1** Parameters of the bamboo scrimber

| Material        | Bending strength (Mpa) | Compressive strength parallel to grain (Mpa) | Compressive strength perpendicular to the grain (MPa) |                       |                           |                           |
|-----------------|------------------------|----------------------------------------------|-------------------------------------------------------|-----------------------|---------------------------|---------------------------|
|                 |                        |                                              | Radial total strength                                 | Radial local strength | Tangential total strength | Tangential local strength |
| Bamboo scrimber | 260                    | 75.5                                         | 24.9                                                  | 13.6                  | 24.2                      | 14.9                      |

128

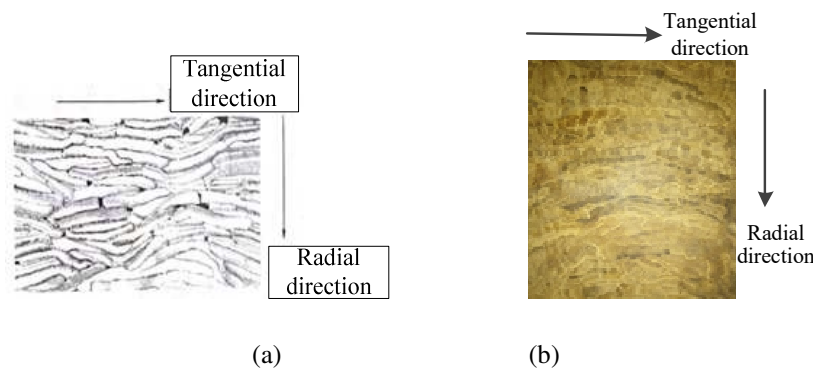
129 Fully threaded STSs with double countersunk head were used in this test. Three screw  
 130 diameters of 6mm, 8mm and 10mm with the same length of 140mm were considered. Table 2  
 131 lists the technical specifications of the screws as provided by the manufacturer.

132 **Table 2** Specification and strengths of STSs

| Specification | Outside diameter (mm) | Root diameter (mm) | Total length (mm) | Thread length (mm) | Head diameter (mm) | Bending yield strength (MPa) | Tension strength (MPa) |
|---------------|-----------------------|--------------------|-------------------|--------------------|--------------------|------------------------------|------------------------|
| FTCD-6        | 6                     | 4                  | 140               | 130                | 11.8               | 1000.0                       | 1100.0                 |
| FTCD-8        | 8                     | 5.3                | 140               | 130                | 15.5               | 1000.0                       | 1100.0                 |

133 2.2 Test specimens and parameters

134 The texture of the bamboo scrimber is similar to that of the engineered wood, so the texture  
135 directions can be defined according to the definitions for parallel strand lumber (PSL) [49].  
136 Since the bamboo slices that form the bamboo scrimber usually have a larger width than the  
137 thickness, the direction along the width of the bamboo slices is defined as the tangential  
138 direction and that along the thickness is defined as radial direction (Fig. 2).



139  
140  
141 **Fig. 2.** Bamboo scrimber sectional definition: (a) PSL Sectional features [30], (b) Bamboo scrimber  
142 Sectional features

143 The specimens were designed in conformation with ASTM D1761 [50] and the Chinese  
144 Standard LY-T2377-2014 [51] for testing fasteners in wood. Three main factors affecting the  
145 withdrawal resistance were investigated, namely, a) effective embedment length  $l_{ef}$ , b) screw  
146 angle relative to grain direction  $\alpha$ , and c) insert texture directions (Group T). Totally 210  
147 specimens were tested with the same type of bamboo scrimber, and these were divided into  
148 three main groups, as follows:

149 Group RD: this group was designed to investigate the effect of the embedment length on  
150 the withdrawal resistance, with the embedment length varying between 20mm, 30mm and  
151 40mm, while the screw angle  $\alpha$  was kept at 90 degrees. Three different screw diameters of



152 6mm, 8mm and 10mm, respectively, were considered. Thus, Group RD actually consisted of  
153 9 series of specimens, as listed in detail in Table 3.

154 Group RA: this group focused on the effect of the insertion angle on the withdrawal  
155 resistance. In addition to the 90° angle already tested in Group RD, two further angles,  
156 namely 0° and 45°, were included. For each angle, three different screw diameters of 6mm,  
157 8mm and 10mm, respectively, were considered. The embedment length was kept constant at  
158 30mm. Thus, 6 new series of specimens were tested in this group.

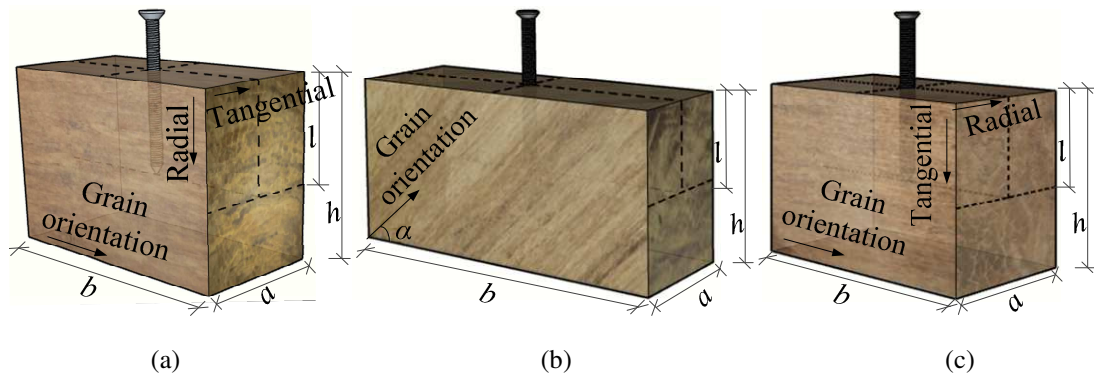
159 Group T: this group was added to test the screw insertion in the tangential direction of  
160 the bamboo scrimber from the section point of view (Fig. 2(b)), in addition to the radial  
161 direction as in Group RD and RA. Two screw angles relative to the grain direction ( $\alpha= 45^\circ$ ,  
162  $90^\circ$ ) and three screw diameters (6mm, 8mm and 10mm) were considered for Group T, making  
163 further 6 series of test specimens as listed also in Table 3.

164 Fig. 3 shows a representative diagram of specimens in three groups. The length, width,  
165 height of the specimens and the screw embedment length are denoted by  $a$ ,  $b$ ,  $h$ , and  $l$   
166 respectively. The effective embedment length,  $l_{ef}$ , is defined by  $l$  minus the length of the screw  
167 tip which is assumed equal to the diameter of the screws,  $d$ ; thus  $l_{ef} = l - d$ . The size  
168 parameters of the specimens are listed in Table 3.

169 The specimens are labelled according to their parameter settings, for example R-6d-90-  
170 20. The first character, R or T, represents that the thrust direction of the self-tapping screw, i.e.,  
171 in the radial direction (R) or tangential direction (T) of the bamboo scrimber. The second part  
172 represents the outer diameter of the STS, with 6d, 8d and 10d denoting 6 mm, 8 mm, and 10  
173 mm of the STS diameter, respectively. The 3<sup>rd</sup> part represents the angle between the axis of

174 the STSs and the bamboo scrimber fiber. For example, 90 means that the STS is driven to the  
 175 bamboo scrimber fiber bundle perpendicularly, and 0 indicates that the axis of STS is the  
 176 same as the direction along the grain of the bamboo (Fig. 4). The 4<sup>th</sup> part denotes the effective  
 177 embedment length of the STS.  $\lambda$  represents the anchoring slenderness ratio, i.e., the ratio of  
 178 the effective embedment length to the diameter of the STS. Prior to the selection of the  
 179 effective embedment lengths for the specimens, a preliminary experiment was carried out to  
 180 determine the baseline value of  $\lambda$  which corresponded to the yield failure of the STSs. Details  
 181 of the preliminary experiment are given in Section 2.1.

182



183

184

185

**Fig. 3.** Test specimens: (a) Group RD, (b) Group RA, (c) Group T

186



187

**Fig. 4.** R-8d-0-30

188

189

It is common practice with wood materials that when the wood density exceeds 0.5 g/cm<sup>3</sup>, the wood needs to be pre-drilled for STSs installation [52]. In the present test, the

190 average density of the bamboo scrimber was 1.05 g/cm<sup>3</sup>, so pre-drilling was considered for  
191 the installation of STSs. For confirmation purpose, a comparative test was firstly carried out  
192 between trial specimens with and without pre-drilling in the installation of the STSs. Test  
193 results showed that the STSs without pre-drilled holes were pulled out earlier with damage in  
194 the thread of the STSs, and the withdrawal resistance was much smaller than that of the STSs  
195 with pre-drilled holes. This indicates that the bamboo scrimber under investigation cannot  
196 provide sufficient holding strength without pre-drilling. Therefore, pre-drilling was adopted in  
197 all the formal test specimens. The diameter of the pre-drilled hole was made no greater than  
198 0.6 times the outer diameter of the STSs [52].

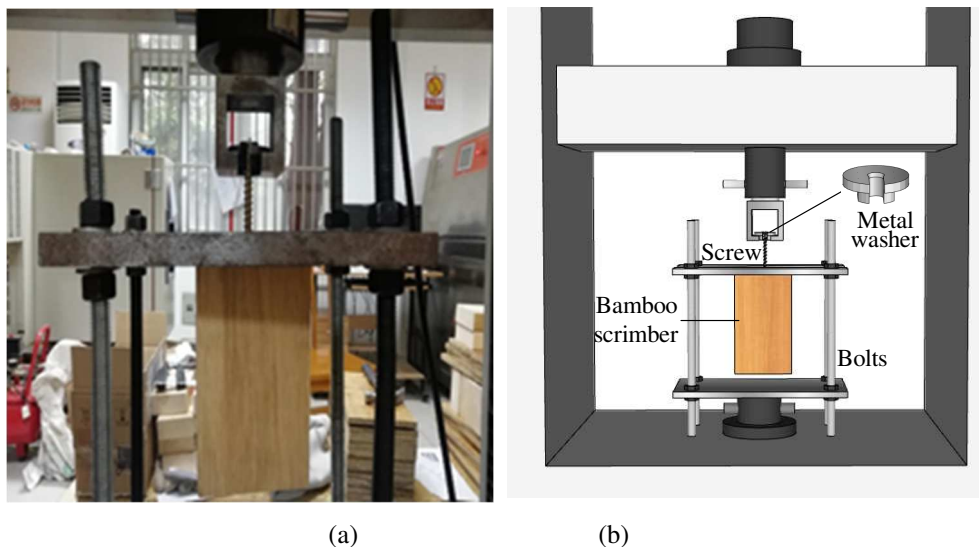
199 **Table 3** Dimensional parameters of the specimens

| Specimens group | Specimens Series | $d$ (mm) | $\alpha$ (°) | $l_{ef}$ (mm) | $a$ (mm) | $b$ (mm) | $h$ (mm) | $\rho$ (g/cm <sup>3</sup> ) | $\lambda$ | $n$ |
|-----------------|------------------|----------|--------------|---------------|----------|----------|----------|-----------------------------|-----------|-----|
| RD              | R-6d-90-20       | 6        | 90°          | 20            | 60       | 120      | 90       | 1.17                        | 3.3       | 10  |
|                 | R-6d-90-30       | 6        | 90°          | 30            | 60       | 120      | 110      | 1.05                        | 5         | 10  |
|                 | R-6d-90-40       | 6        | 90°          | 40            | 60       | 120      | 130      | 1.05                        | 6.6       | 10  |
|                 | R-8d-90-20       | 8        | 90°          | 20            | 80       | 160      | 100      | 1.07                        | 2.5       | 10  |
|                 | R-8d-90-30       | 8        | 90°          | 30            | 80       | 160      | 120      | 1.01                        | 3.75      | 10  |
|                 | R-8d-90-40       | 8        | 90°          | 40            | 80       | 160      | 140      | 1.04                        | 5         | 10  |
|                 | R-10d-90-20      | 10       | 90°          | 20            | 100      | 200      | 110      | 1.05                        | 2         | 10  |
|                 | R-10d-90-30      | 10       | 90°          | 30            | 100      | 200      | 130      | 1.02                        | 3         | 10  |
|                 | R-10d-90-40      | 10       | 90°          | 40            | 100      | 200      | 150      | 1.04                        | 4         | 10  |
| RA              | R-6d-0-30        | 6        | 0°           | 30            | 60       | 60       | 110      | 1.05                        | 5         | 10  |
|                 | R-6d-45-30       | 6        | 45°          | 30            | 130      | 60       | 130      | 1.09                        | 5         | 10  |
|                 | R-8d-0-30        | 8        | 0°           | 30            | 80       | 80       | 120      | 0.97                        | 3.75      | 10  |
|                 | R-8d-45-30       | 8        | 45°          | 30            | 160      | 80       | 130      | 1.01                        | 3.75      | 10  |
|                 | R-10d-0-30       | 10       | 0°           | 30            | 100      | 100      | 130      | 1.04                        | 3         | 10  |
|                 | R-10d-45-30      | 10       | 45°          | 30            | 200      | 100      | 130      | 1.01                        | 3         | 10  |
| T               | T-6d-90-30       | 6        | 90°          | 30            | 60       | 120      | 110      | 1.05                        | 5         | 10  |
|                 | T-8d-90-30       | 8        | 90°          | 30            | 80       | 160      | 120      | 1.05                        | 3.75      | 10  |
|                 | T-10d-90-30      | 10       | 90°          | 30            | 100      | 200      | 130      | 1.04                        | 3         | 10  |
|                 | T-6d-45-30       | 6        | 45°          | 30            | 130      | 60       | 130      | 1.24                        | 5         | 10  |
|                 | T-8d-45-30       | 8        | 45°          | 30            | 160      | 80       | 130      | 1.22                        | 3.75      | 10  |
|                 | T-10d-45-30      | 10       | 45°          | 30            | 200      | 100      | 130      | 1.19                        | 3         | 10  |

200 Note:  $d$ ,  $l_{ef}$  denotes the outside diameter, the effective embedment length into the member of the  
201 STSs;  $\alpha$  denotes the angle between the axial of STSs and the grain;  $\rho$  and  $n$  denote the density and  
202 number of the specimens.

203 2.3 Test method

204 The test was conducted using a 100kN mechanical testing machine. The bamboo scrimber  
205 specimen was fixed on the testing machine with a dowel-connected special fixture, and the  
206 head of the STSs was fixed to the loading head of the testing machine with metal washers and  
207 bolts. The loading configuration is shown in Fig. 5. According to ASTM D5652 [53], the  
208 displacement control method at the rate of loading of 3 mm/min was adopted. The actual  
209 loading time for each test piece was 3~5 min and the loading was terminated when the test  
210 piece broke or the load-displacement curve developed a significant drop. In the test, the load  
211 and displacement were measured and recorded by the MTS force sensor and displacement  
212 sensor.



215 **Fig. 5.** Test setup: (a) specimen under testing, (b) schematic of setup

216 **3 Test results and analysis**

217 3.1 Preliminary test

218 To determine an appropriate range of embedding length, a preliminary test was designed and  
219 carried out ahead of the formal test. In the preliminary test group, tests were performed on the

220 specimens with anchoring slenderness ratios  $\lambda$  of 6, 7, and 8.

221       When the values of  $\lambda$  were 6 and 7, the specimen behaved in an elastic manner at the  
222 initial stage, with no obvious damage. Beyond a certain elastic limit, the load increased at  
223 reduced rates with increase of the displacement, showing inelastic behaviours which were  
224 accompanied with slight bamboo fibre fracture sound. When the loading reached the  
225 maximum level, a rapid decrease of the load was followed with an apparent sound of wood  
226 breaking. During the whole process, the screw was in the elastic stage and there was no  
227 yielding failure. When the value of  $\lambda$  was 8, the specimens exhibited a similar general  
228 behaviour as described above. However, when the loading reached a certain level, the screw  
229 ruptured at the end region with a loud bang (Fig. 6), marking a total failure of the specimens.  
230 By further narrowing the range of  $\lambda$ , it was found that  $\lambda$  equal to 7.5 approximately marked a  
231 critical embedment length; a longer embedment length would lead to the rupture of the STSs,  
232 whereas a shorter embedment length would generally guarantee an STS pull-out failure.

233       For STS of a diameter of 6mm, the embedment length for  $\lambda=7.5$  is 45mm. Finally, the  
234 test embedment lengths of the STSs were determined as 20mm, 30mm, and 40mm for STS  
235 specimens of all three diameters to ensure a pull-out mode of failure. As will be presented in  
236 the test results later, all of the specimens did exhibit an STS pull-out failure, enabling the  
237 determination of the STS withdrawal resistance of the specimens.



238

239

**Fig. 6.** Rupture failure of the STSs for  $\lambda=7.5$

### 240 3.2 General response and failure mode

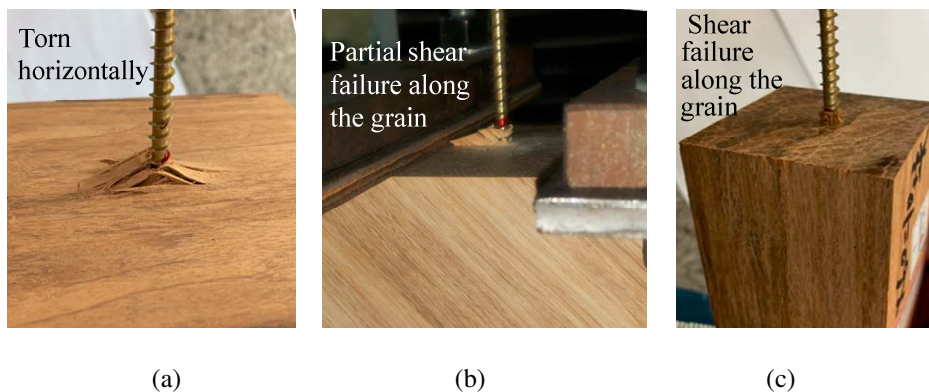
241 The performance of each specimen was similar before the attainment of the ultimate bearing  
242 capacity. During the initial loading stage, the anchoring surface of the restructured bamboo  
243 remained intact (Fig. 7a), and the load increased linearly with the displacement. After the  
244 displacement reached a certain level, the increasing rate of the load decreased, while a slight  
245 bamboo tearing sound was heard. When the loading approached the withdrawal resistance of  
246 the STSs, the relative slip became pronounced and this was accompanied by the bamboo fibre  
247 fracture sound (Fig. 7b).

248 After reaching the ultimate bearing capacity, all specimens exhibited a pull-out failure of  
249 the STSs. Due to a different angle  $\alpha$  between the pull-out force of the STSs and the bamboo  
250 scrimber bundle, different groups of specimens showed different failure modes. In the RD  
251 group and the T group with  $\alpha=90^\circ$ , the bamboo fiber was torn horizontally. In the later stage  
252 of loading, the load reduction rate was stable, and a certain residual withdrawal capacity  
253 remained (Fig. 8a). In the RA group with  $\alpha=45^\circ$ , the affected part of the bamboo scrimber  
254 fiber underwent shear failure along the grain. In the later stage of loading, the load dropped  
255 faster than the specimens in the former two groups with  $\alpha=90^\circ$  and the residual withdrawal  
256 capacity was smaller (Fig. 8b). In the RA group with  $\alpha=0^\circ$ , the bamboo fiber bundle

257 underwent shear along the grain and was pulled out together with the STSs. After the ultimate  
258 bearing capacity, the load dropped rapidly (Fig. 8c). It is worth noting that in the special case  
259 where the STS was nailed at the glue layer, the failure mode was that the reorganized bamboo  
260 split along the glue joint. Therefore, for  $\alpha=0^\circ$ , the nailing position should be kept sufficiently  
261 away from the glue joint.



264 **Fig. 7.** Specimens under loading: (a) Initial stage of loading, (b) Approaching peak load



267 **Fig. 8.** Typical failure modes for different insertion angles: (a)  $90^\circ$ , (b)  $45^\circ$ , (c)  $0^\circ$

### 268 3.3 Withdrawal resistance

269 With reference to the law of lognormal distribution of wood strength [54], the  
270 withdrawal resistance of STSs is analyzed using the lognormal distribution herein. The  
271 withdrawal resistance results of the test specimens are shown in Table 4, including the  
272 distribution parameters. A comparison between the probability distribution curves of predicted  
273 data and test data is shown in Figs. 9 - 11.

274 As shown in Table 4, the average value and the 5<sup>th</sup> percentile value of the withdrawal  
275 resistance in the RD group gradually increase with the increase of the embedment length.  
276 Especially, the 5<sup>th</sup> percentile value increases linearly with the embedment length (Fig. 9). The  
277 withdrawal resistance of the RD group also increases with the increase of the diameter of  
278 STSs. It is noted that the average withdrawal resistance of the STSs with a diameter of 6mm  
279 (R-6d-90-20) is greater than the diameter of 8mm (R-8d-90-20). In addition to the larger  
280 density of the R-6d-90-20 series, the main reason is that the anchor slenderness ratio  $\lambda$  of the  
281 latter two series (R-8d-90-20, R-10d-90-20) is markedly small. The small value of  $\lambda$  affects  
282 the development of the withdrawal resistance of STSs, and based on the present observation it  
283 is recommended that the minimum  $\lambda$  of the STSs in bamboo scrimber is 3.

284 Table 4 also shows that the average withdrawal resistance of the STSs with  $\alpha=45^\circ$  in the  
285 RA group is greater than that of the specimens with  $\alpha=0^\circ$ . Comparison with the RD group  
286 and the T group implies that the withdrawal resistance of the STSs driven in the radial or  
287 tangential direction is greater than that of the STSs driven along the grain. This is consistent  
288 with experimental observations from the literature [37] in that the withdrawal resistance of the  
289 STSs increases as the angle  $\alpha$  between the STSs and the bamboo fiber increases. The main  
290 reason is that with an increase of the angle more bamboo fibers become intertwined with the  
291 STSs, resulting in less grain-wise shear damage of bamboo fiber and more horizontal grain  
292 shear damage.

293 For group T, the average value and the 5<sup>th</sup> percentile value of the withdrawal resistance  
294 of the STSs in the tangential direction increase with the increase of the diameter. This is  
295 consistent with the increase of the contact area between the STSs and the bamboo scrimber.



296 However, it is noted that because the average density of the specimens with  $\alpha=45^\circ$  in the  
 297 tangential direction is about 17% larger than that of the ones with  $\alpha=90^\circ$  (Table 1), the  
 298 average withdrawal resistance of the STSs with  $\alpha=45^\circ$  is higher. This shows that the density  
 299 of bamboo scrimber has a certain effect on the anchoring capacity of self-tapping screws,  
 300 similar to wood.

301

302

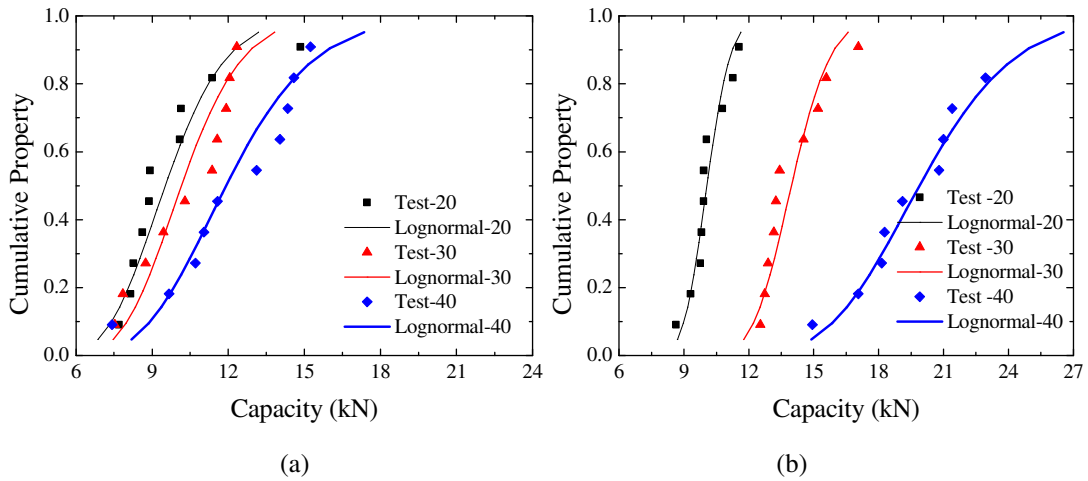
**Table 4.** Withdrawal resistance and stiffness of the STSs

| Test group | Test series | Mean                       |                   | Withdrawal resistance (Lognormal distribution, kN) |          |       | Stiffness (Normal distribution, kN/mm) |          |      |
|------------|-------------|----------------------------|-------------------|----------------------------------------------------|----------|-------|----------------------------------------|----------|------|
|            |             | Withdrawal resistance (kN) | Stiffness (kN/mm) | St.dev                                             | Cov. (%) | 5th   | St.dev                                 | Cov. (%) | 5th  |
| RD         | R-6d-90-20  | 9.70                       | 4.0               | 0.20                                               | 8.7      | 6.86  | 0.40                                   | 10.1     | 3.33 |
|            | R-6d-90-30  | 10.31                      | 4.42              | 0.18                                               | 8.0      | 7.47  | 0.50                                   | 11.4     | 3.58 |
|            | R-6d-90-40  | 12.17                      | 4.22              | 0.22                                               | 9.1      | 8.18  | 0.57                                   | 13.6     | 3.26 |
|            | R-8d-90-20  | 6.21                       | 3.82              | 0.24                                               | 13.1     | 4.07  | 0.80                                   | 21.1     | 2.47 |
|            | R-8d-90-30  | 13.50                      | 5.19              | 0.22                                               | 8.5      | 9.15  | 0.60                                   | 11.6     | 4.18 |
|            | R-8d-90-40  | 17.92                      | 5.35              | 0.23                                               | 8.2      | 11.83 | 0.63                                   | 11.8     | 4.29 |
|            | R-10d-90-20 | 10.09                      | 4.48              | 0.09                                               | 3.7      | 8.70  | 0.29                                   | 6.4      | 4.0  |
|            | R-10d-90-30 | 14.04                      | 5.43              | 0.10                                               | 4        | 11.76 | 0.72                                   | 13.3     | 4.24 |
|            | R-10d-90-40 | 20.16                      | 5.84              | 0.17                                               | 5.8      | 14.9  | 0.54                                   | 9.3      | 4.93 |
| RA         | R-6d-0-30   | 8.24                       | 4.25              | 0.33                                               | 16.3     | 4.46  | 0.72                                   | 16.9     | 3.05 |
|            | R-6d-45-30  | 11.38                      | 4.80              | 0.13                                               | 5.2      | 9.15  | 0.28                                   | 5.79     | 4.33 |
|            | R-8d-0-30   | 9.08                       | 4.13              | 0.21                                               | 9.6      | 6.28  | 0.61                                   | 14.9     | 3.10 |
|            | R-8d-45-30  | 13.25                      | 4.71              | 0.20                                               | 7.8      | 9.31  | 0.77                                   | 16.3     | 3.43 |
|            | R-10d-0-30  | 10.76                      | 4.86              | 0.20                                               | 8.3      | 7.62  | 0.51                                   | 10.5     | 4.01 |
|            | R-10d-45-30 | 15.59                      | 5.97              | 0.11                                               | 4.0      | 12.89 | 0.80                                   | 13.4     | 4.64 |
| T          | T-6d-90-30  | 10.72                      | 4.85              | 0.25                                               | 10.6     | 6.88  | 0.49                                   | 10.2     | 4.02 |
|            | T-8d-90-30  | 13.36                      | 5.31              | 0.23                                               | 8.8      | 8.94  | 0.66                                   | 12.4     | 4.21 |
|            | T-10d-90-30 | 14.62                      | 5.27              | 0.12                                               | 4.4      | 11.92 | 0.51                                   | 9.6      | 4.42 |
|            | T-6d-45-30  | 14.98                      | 5.74              | 0.15                                               | 5.6      | 11.54 | 0.41                                   | 7.2      | 5.05 |
|            | T-8d-45-30  | 17.25                      | 6.40              | 0.17                                               | 5.8      | 13.1  | 0.79                                   | 12.4     | 5.25 |
|            | T-10d-45-30 | 21.94                      | 7.15              | 0.13                                               | 4.2      | 17.6  | 0.54                                   | 7.6      | 6.25 |

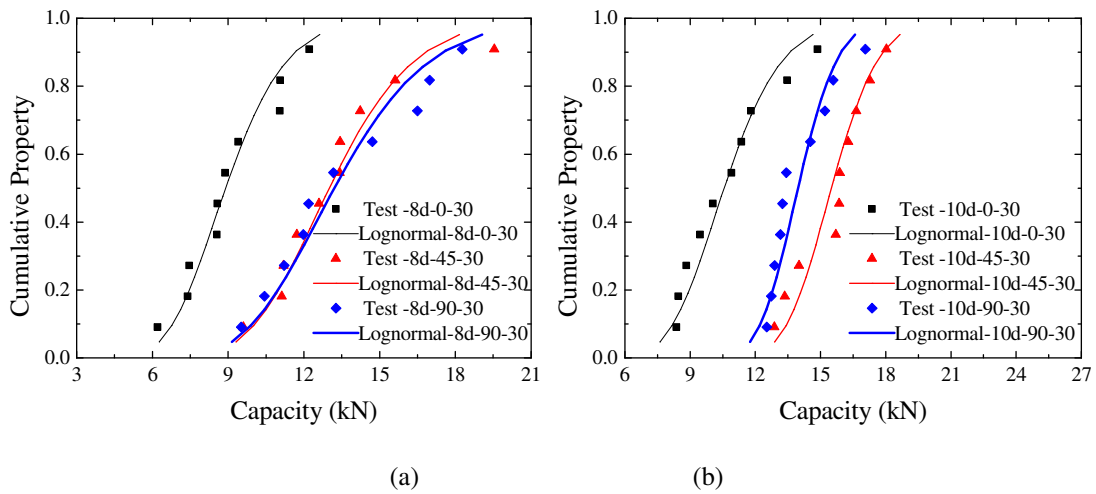
303

304 From the comparison of the RD and RA groups in Fig. 10, it can be observed that the 5<sup>th</sup>  
 305 percentile value of the withdrawal resistance of STSs with  $\alpha=45^\circ$  is close to that of specimens  
 306 with  $\alpha=90^\circ$ . This is different from the behavior of the withdrawal resistance of STSs in

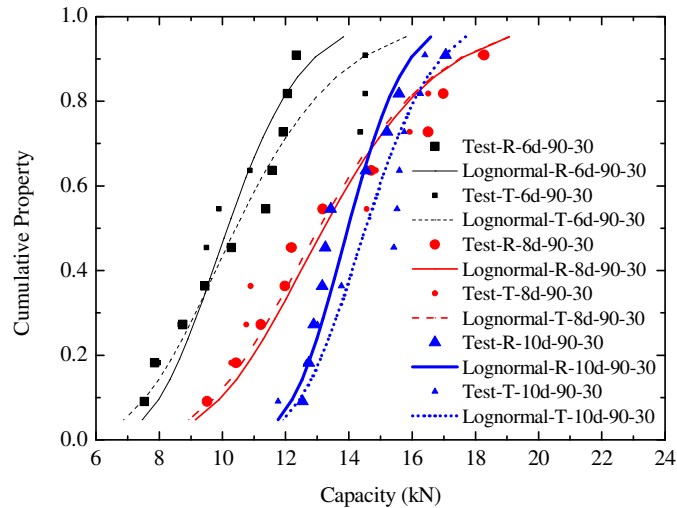
307 wooden structures. Fig. 11 shows that the 5th percentile values of the withdrawal resistance of  
 308 STSs in the radial and tangential directions are very close, and the average relative difference  
 309 is less than 2.3% (Table 4).



310  
 311 (a) (b)  
 312 **Fig.9.** Comparison between a fitted distribution and test data in Group RD: (a) R-6d-90, (b) R-10d-90



314 (a) (b)  
 315  
 316 **Fig. 10.** Comparison between a fitted distribution and test data in Group RD and Group RA: (a) R-8d,  
 317 (b) R-10d



318

319 **Fig.11.** Comparison between a fitted distribution and test data in Group RD and Group RA

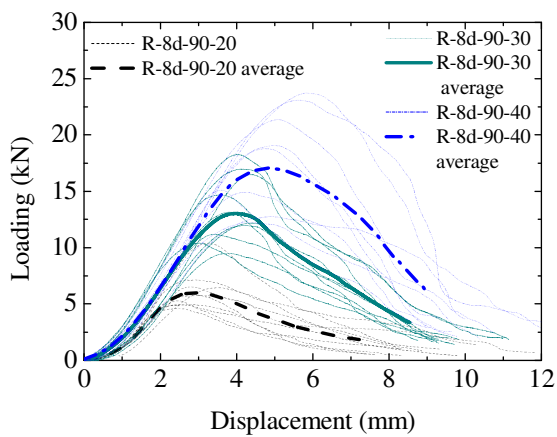
320 3.4 Load-displacement curves

321 The global performance of the STSs in the bamboo scrimber can be illustrated clearly in the  
 322 load-displacement curves. Figs. 12 show the load-displacement curves of the three groups and  
 323 the average curve of each series. In the initial stage of loading, the curves are approximately  
 324 linear, indicating the withdrawal force is in the elastic stage. Nonlinear response develops as  
 325 the displacement increases beyond a certain elastic limit. Approaching the peak load, the  
 326 specimens generally exhibit a certain degree of permanent deformation.

327 The RD group (Figs. 12a, 12b) shows that the withdrawal resistance capacity of STSs  
 328 and the slope of the descending branch increases as the embedment length increases. The  
 329 increase in the diameter of the STSs also causes similar effects. This is because with a larger  
 330 diameter the contact area between an STS and the bamboo scrimber is larger, leading to a  
 331 larger wedge body that is formed by the extrusion of the STS from the bamboo scrimber.  
 332 Hence, the withdrawal resistance increases. In Fig. 12, a few curves with smaller embedment  
 333 lengths appear above the curves with larger embedment lengths, and this is attributable to the  
 334 scatter of the properties of the specimens.

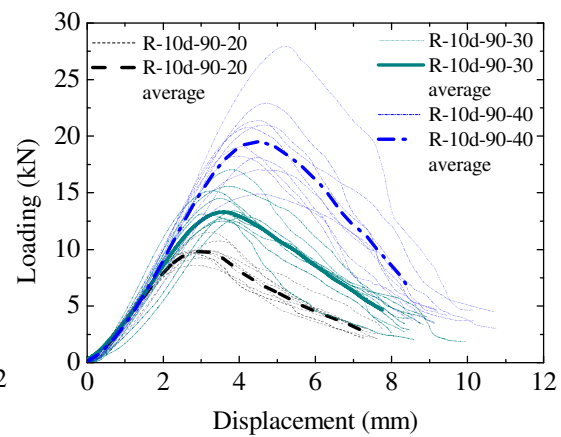
335 A comparison of the load-displacement curves corresponding to the three angles in the  
 336 RD and RA groups is presented in Figs. 12c, 12d. The ultimate bearing capacity increases as  
 337 the angle increases. This is consistent with the failure mode of the STSs in the test in that the  
 338 smaller the angle, the more likely that the bamboo fibers bundled around the STS will  
 339 undergo shear failure along the grain, giving rise to the characteristics of more brittle failure.

340 The load-displacement curves of the T group and the RD group are plotted in Figs. 12e,  
 341 12f. The main trend of load-displacement curves in the radial and tangential directions is  
 342 similar. However, since the arrangement of bamboo fiber bundles is slightly different, the  
 343 load-displacement curves in the tangential direction tend to be steeper than the radial curves.

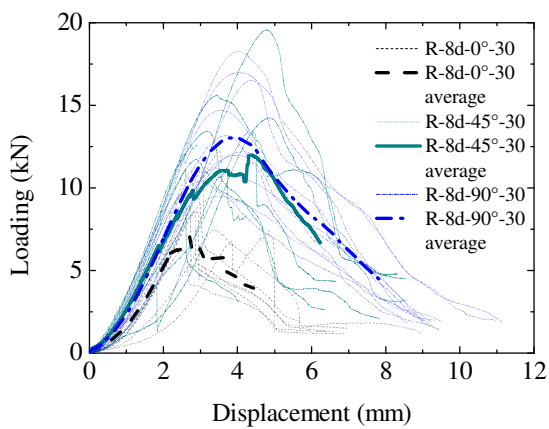


344  
345

(a)

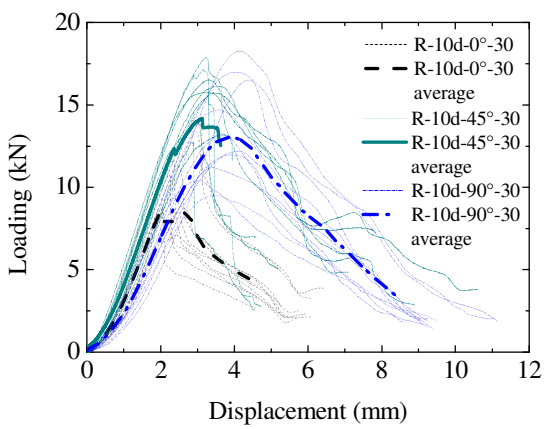


(b)

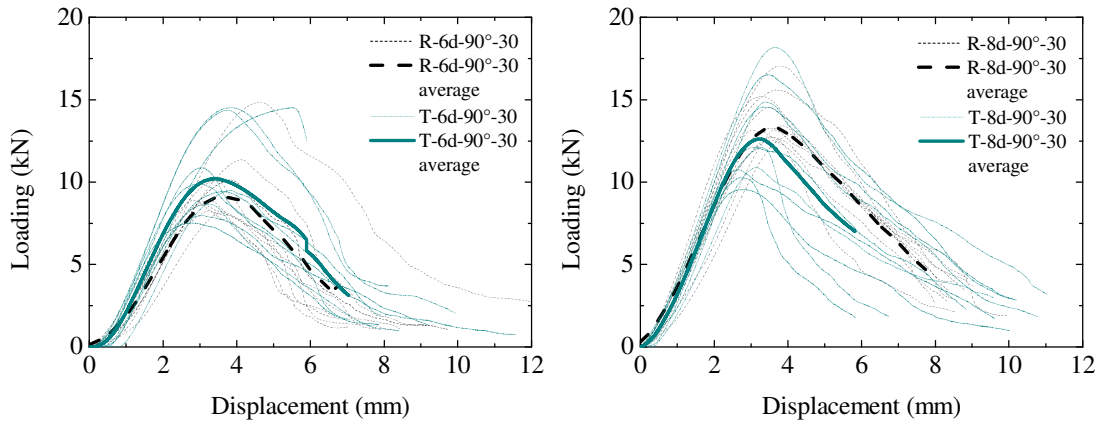


346  
347

(c)



(d)



348

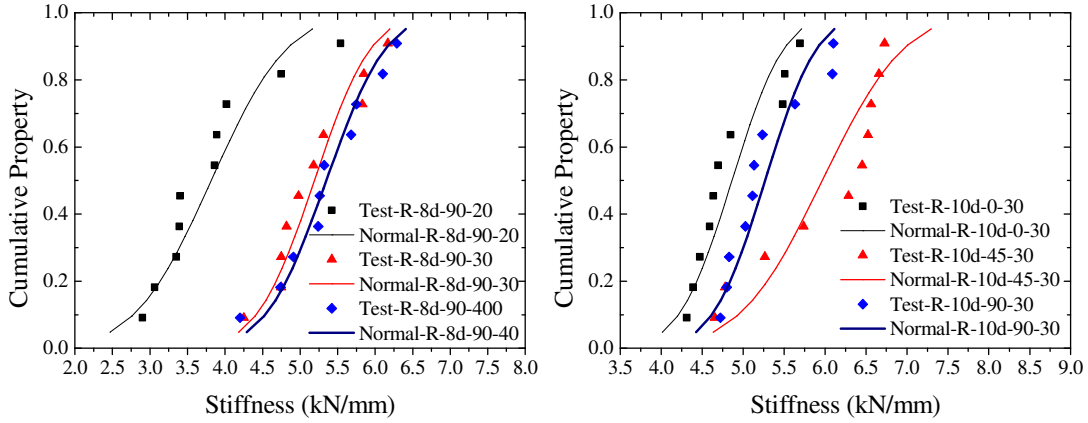
(e)

(f)

349  
 350 **Fig. 12.** Load-displacement curves: (a) RD group,  $d=8\text{mm}$ , (b) RD group,  $d=10\text{mm}$ , (c) RD group,  
 351  $d=8\text{mm}$  with three angles, (d) RD group,  $d=10\text{mm}$  with three angles, (e) T group and RD group,  
 352  $d=6\text{mm}$ , (f) T group and RD group,  $d=8\text{mm}$ .

353 3.5 Withdrawal stiffness

354 The slope of the load-slip curves from 2kN to 4kN, within the generally linear range, is  
 355 adopted to represent the stiffness of the specimens. Again with reference to the law of  
 356 lognormal distribution of the stiffness of wood [54], the withdrawal stiffness of STSs is  
 357 analyzed using normal distribution herein. The withdrawal stiffness results of the test  
 358 specimens and the distribution parameters are included in Table 4. It can be seen that the  
 359 withdrawal stiffness of the STSs increases with the increase of the embedment length, the  
 360 diameter of the STSs, and the screw angle. This is similar to the rule of the withdrawal  
 361 resistance as shown in Fig. 12 and Fig.13.



362

363

364 **Fig.13.** Comparison between a fitted distribution and test data of withdrawal resistance: (a) R-8d-90, (b)

365 R-10d

## 366 4 Calculation of withdrawal resistance of STSs in bamboo scrimber

367 4.1 Existing calculation methods for withdrawal resistance of STSs in wood and raw

368 bamboo

369 At present, Eurocode 5 [41] and industry standards (e.g. CCMC 13677-R [42]) provide

370 the calculation formulas for the 5<sup>th</sup> percentile value of withdrawal resistance of STSs in wood

371 for application in the design. The calculation formula in Eurocode 5 [41] are as follows:

$$372 F_{ax,k,Rk} = \frac{n_{ef} f_{ax,k} d \cdot l_{ef} \cdot k_d}{1.2 \cos^2 \alpha + \sin^2 \alpha} \quad (1)$$

$$373 f_{ax,k} = 0.52 d^{-0.5} l_{ef}^{-0.1} \cdot \rho_k^{0.8} \quad (2)$$

374 where  $F_{ax,k, Rk}$  is the characteristic withdrawal force capacity of the connection at an angle  $\alpha$  to

375 the grain, in N;  $f_{ax,k}$  is the characteristic withdrawal resistance perpendicular to the grain, in

376 N/mm<sup>2</sup>;  $n_{ef}$  is the effective number of screws;  $l_{ef}$  is the penetration length of the threaded part,

377 in mm;  $\rho_k$  is the characteristic density, in kg/m<sup>3</sup>;  $\alpha$  is the angle between the screw axis and the

378 grain direction;  $k_d$  is the diameter parameter, taking the smaller value of 1 and  $d/8$ , in mm.

379 The calculation formula specified in CCMC 13677-R [42] is expressed as:

380 
$$P_{rw,\alpha} = \phi \frac{0.8\delta(b \cdot 0.84 \cdot \rho)^2 \cdot d \cdot l_{ef} \cdot 10^{-6}}{\sin^2 \alpha + \frac{4}{3} \cdot \cos^2 \alpha} \cdot K_D \cdot K_{SF} \quad (3)$$

381 where  $P_{rw,\alpha}$  is factored withdrawal resistance for installation angle  $\alpha$ ;  $\phi$  is the resistance factor  
 382 for design purpose,  $\phi=0.9$ ; 0.8 is load duration normalization factor and is applied to adjust  
 383 to standard term loading;  $\delta$  is material adjustment factor:  $\delta=82$  for  $\rho \geq 440\text{kg/m}^3$ ,  $\delta =85$  for  $\rho$   
 384  $<440\text{kg/m}^3$ ;  $b$  is the material factor:  $b=1$  for D-Fir-L, SPF, SYP, STP, WRC, Hem-Fir,  
 385  $b=0.75$  for Parallam (PSL);  $\rho$ =mean oven-dry relative density (CSA O86, Table A.10.1)  $\times 10^3$   
 386  $\text{kg/m}^3$ ; 0.84 is the adjustment of mean oven-dry relative to fifth percentile value;  $d$  is the  
 387 outside screw diameter (mm);  $l_{ef}$  is the effective embedment length into the member:  $l_{ef} =$   
 388 thread length - tip length ( $=d$ ) (mm);  $K_D$  and  $K_{SF}$  are the load duration factor and service  
 389 condition factor, respectively.

390 For the withdrawal resistance of STSs in the raw bamboo, an empirical formula has been  
 391 proposed [43], which is similar to the calculation formula given by Eurocode 5 [41] but with  
 392 improved accuracy when applied to calculate the screw withdrawal capacity in raw bamboo  
 393 [43].

#### 394 4.2 Calculation of the withdrawal resistance of STS in bamboo scrimber

395 Based on the analysis of the experimental performance and the withdrawal resistance of STSs  
 396 in bamboo scrimber in Section 3.3, the effects of the pertinent parameters, including the  
 397 embedment length, screw diameter and embedment angle, are very similar to the situation  
 398 with STSs in wood. Therefore, the formulas of Eurocode 5 and CCMC (2013) are firstly used  
 399 to calculate the characteristic value of the withdrawal resistance of STS in bamboo scrimber.

400 The calculation results are compared with the 5<sup>th</sup> percentile value of withdrawal resistance of

401 STSs in the tests. Considering the dispersion of the bamboo scrimber properties, a lognormal  
402 distribution with a coefficient of variation of 20% is assumed in this paper [35]. Based on this  
403 coefficient, the average value of the withdrawal capacity is estimated.

404 The above two calculated values are compared with the test results in Table 5. Note that  
405 the comparisons are given for cases with  $\lambda \geq 3$ , taking into consideration that smaller  $\lambda$   
406 appeared to be inadequate to ensure an effective withdrawal resistance of STSs, as mentioned  
407 earlier in Section 3.4. Furthermore, in the calculation of the withdrawal resistance of STS  
408 using Eq. (3), factors for the purpose of design, including the resistance factor  $\phi$  and service  
409 condition factor  $K_{SF}$ , are set equal to 1.0. The material factor  $b$  is set equal to 0.75, which is  
410 taken from the engineering wood SPL. Since the experiment involved short-term loads, the  
411 load duration adjustment factor  $K_D$  is set at 1.25 for short-term loading [55].

412 The comparison results in Table 5 show that, in terms of the characteristic values, the  
413 withdrawal resistance calculated by Eurocode 5 (equations 1-2) exhibit an average error of 26%  
414 relative to the test results, whereas the results calculated using the CCMC 13677-R formula  
415 (equation 3) give an average relative error of 16%. In terms of the average withdrawal  
416 resistance, the results calculated using Eurocode 5 (equations 1-2) give an average error of  
417 about 18% as compared to an average error of 12% when equation 3 is employed.

418 Besides, the average relative error between the characteristic value calculated with the  
419 empirical formula for raw bamboo [43] and the test result of the first three series of specimens  
420 with  $\alpha=90^\circ$  in the RD group and the T group is 18%. The average relative error between the  
421 average value calculated with the same empirical formula [43] and the test result is 6% and  
422 the maximum relative error is 39%. This suggests that the accuracy of equation 3 for the



423 withdrawal resistance of STS in bamboo scrimber is better than the Eurocode 5 formula and  
 424 empirical formula for raw bamboo [43].

425 **Table 5** Comparison of withdrawal resistance between calculated values and test results [kN]

| Specimens   | Test result                   |       | EN1995        |            |                      |            | CCMC            |            |                      |            |
|-------------|-------------------------------|-------|---------------|------------|----------------------|------------|-----------------|------------|----------------------|------------|
|             | 5 <sup>th</sup><br>percentile | mean  | $F_{ax,k,Rk}$ | $\Delta^a$ | Estimated<br>average | $\Delta^b$ | $P_{rw,\alpha}$ | $\Delta^a$ | Estimated<br>average | $\Delta^b$ |
| R-6d-90-20  | 6.86                          | 9.7   | 4.36          | 0.36       | 6.50                 | 0.33       | 6.68            | 0.03       | 9.96                 | 0.03       |
| R-6d-90-30  | 7.47                          | 10.31 | 5.95          | 0.20       | 8.86                 | 0.14       | 8.07            | 0.08       | 12.03                | 0.14       |
| R-6d-90-40  | 8.18                          | 12.17 | 7.45          | 0.09       | 11.10                | 0.09       | 10.76           | 0.32       | 16.04                | 0.24       |
| R-8d-90-30  | 9.15                          | 13.5  | 9.01          | 0.02       | 13.42                | 0.01       | 9.96            | 0.09       | 14.84                | 0.09       |
| R-8d-90-40  | 11.83                         | 17.92 | 11.39         | 0.04       | 16.98                | 0.05       | 14.08           | 0.19       | 20.98                | 0.15       |
| R-10d-90-30 | 11.76                         | 14.04 | 8.29          | 0.30       | 12.35                | 0.12       | 12.70           | 0.08       | 18.92                | 0.26       |
| R-10d-90-40 | 14.9                          | 20.16 | 11.24         | 0.25       | 16.75                | 0.17       | 17.60           | 0.18       | 26.23                | 0.23       |
| R-6d-0-30   | 4.46                          | 8.24  | 4.19          | 0.06       | 6.24                 | 0.24       | 5.94            | 0.33       | 8.85                 | 0.07       |
| R-8d-0-30   | 6.28                          | 9.08  | 4.73          | 0.48       | 7.05                 | 0.38       | 6.89            | 0.10       | 10.27                | 0.12       |
| R-10d-0-30  | 7.62                          | 10.76 | 6.15          | 0.02       | 9.16                 | 0.01       | 9.90            | 0.30       | 14.75                | 0.27       |
| R-6d-45-30  | 6.88                          | 10.72 | 6.94          | 0.25       | 10.34                | 0.22       | 8.07            | 0.17       | 12.03                | 0.11       |
| R-8d-45-30  | 8.94                          | 13.36 | 6.75          | 0.11       | 10.07                | 0.06       | 10.76           | 0.20       | 16.04                | 0.17       |
| R-10d-45-30 | 11.92                         | 14.62 | 7.82          | 0.39       | 11.66                | 0.25       | 13.20           | 0.11       | 19.67                | 0.26       |
| T-6d-90-30  | 6.88                          | 10.72 | 4.92          | 0.29       | 7.33                 | 0.32       | 7.46            | 0.18       | 11.11                | 0.02       |
| T-8d-90-30  | 8.94                          | 13.36 | 7.70          | 0.14       | 11.47                | 0.14       | 8.54            | 0.08       | 12.72                | 0.04       |
| T-10d-90-30 | 11.92                         | 14.62 | 8.18          | 0.31       | 12.19                | 0.17       | 10.67           | 0.17       | 15.90                | 0.02       |
| T-6d-45-30  | 11.54                         | 14.98 | 5.32          | 0.42       | 11.38                | 0.25       | 9.65            | 0.16       | 14.38                | 0.04       |
| T-8d-45-30  | 13.11                         | 17.52 | 8.24          | 0.11       | 13.25                | 0.24       | 12.52           | 0.05       | 18.66                | 0.06       |
| T-10d-45-30 | 17.59                         | 21.94 | 8.90          | 0.31       | 15.59                | 0.26       | 14.81           | 0.16       | 22.08                | 0.01       |

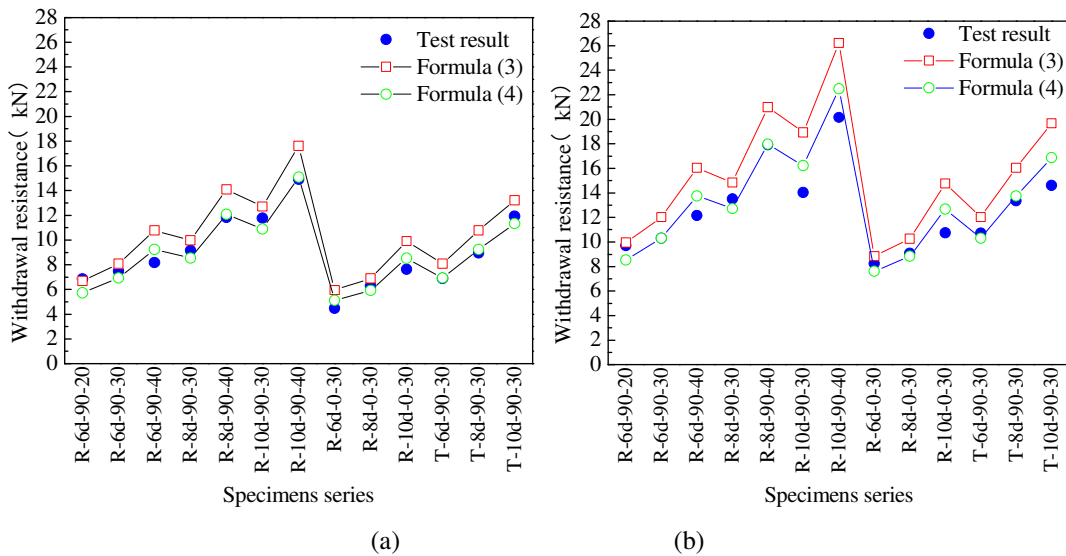
426  
 427 Compared with natural and engineered wood, the bamboo scrimber belongs to a different  
 428 biomass composite material. It is therefore reasonable to expect that, while the basic form of  
 429 the CCMC 13677-R formula may be applied, appropriate modifications are needed so that the  
 430 formula can predict better the withdrawal resistance of STS in bamboo scrimber. Following a  
 431 statistical analysis, a new pair of coefficients for the sine and cosine terms are determined,  
 432 and subsequently the formula is modified into the following expression:

$$433 \quad P_{rw,\alpha} = \frac{1.25\delta(b \cdot 0.84 \cdot \rho)^2 \cdot d \cdot l_{ef} \cdot 10^{-6}}{1.08 \sin^2 \alpha + 1.55 \cos^2 \alpha} \quad (4)$$

434 where,  $P_{rw,\alpha}$  represents the factored withdrawal resistance of STS at an angle of  $\alpha$  to the  
 435 bamboo scrimber fiber; 1.25 is the load duration factor of Eq. (3) converted into the test short-

436 term for the standard period;  $\delta$  is the material adjustment parameter, and the value is 82;  
 437  $b=0.75$  is the material parameter for the bamboo scrimber;  $\rho$  is the average density in  $\text{kg/m}^3$ ;  
 438 0.84 is the adjustment of mean to fifth percentile value;  $d$  is the outside screw diameter of the  
 439 STS in mm;  $l_{ef}$  is the effective embedment length into the member in mm.

440 The relative errors in the calculation results using Eq. (4) relative to the test results for  
 441 angles  $\alpha = 90^\circ$  and  $0^\circ$  are 7% for the 5<sup>th</sup> percentile value and 8% for the average value, as  
 442 illustrated in Fig. 14. A marked improvement of the accuracy as compared to using the  
 443 Eurocode 5 and CCMC 13677-R formulas is observed. Therefore, it is recommended that the  
 444 modified Eq. (4) be used to calculate both the 5<sup>th</sup> percentile and the average values of the  
 445 withdrawal resistance of STS in bamboo scrimber for  $\alpha=90^\circ$  and  $\alpha=0^\circ$ .



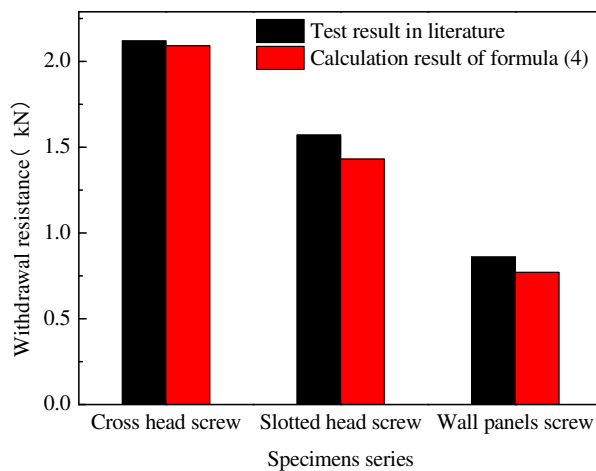
446  
 447  
 448 Fig.14 Comparison of the experimental and calculated withdrawal resistance results: (a) 5th percentile  
 449 value, (b) Average

450 4.3 Verification of the calculation formula

451 To further examine the accuracy of Eq. (4), the experimental results of the withdrawal  
 452 resistance for three kinds of STSs in bamboo scrimber in the literature [21] are selected for  
 453 comparison and verification. The outer diameter of the STSs from the experimental study [21]

454 was 3.5mm. Since the ratio of the pre-drilled hole to the outer diameter of STS has been set at  
 455 approximately 0.6 in the present tests, the test results from the literature with a ratio of the  
 456 pre-drilled hole to the outer diameter close to 0.6 are selected for comparison. Furthermore, it  
 457 is assumed that the coefficient of variation of the withdrawal resistance of the STSs is 20%  
 458 [35].

459 The experimental results of the withdrawal resistance of cross-head screws, slotted  
 460 screws and wall panels screws are 2.12 kN, 1.57 kN and 0.86 kN, respectively. The  
 461 calculation results of these three types of screws using Eq. (4) are found to be 2.06 kN, 1.43  
 462 kN and 0.77 kN, respectively, giving rise to an average error of 8% and maximum error of  
 463 12%, as shown in Fig. 15. This comparison shows that the modified formula in Eq.(4) can  
 464 predict the withdrawal resistance of STSs in bamboo scrimber with good accuracy.



465  
 466 Fig. 15 The comparison of the test result and the calculation result in literature [21]

## 467 5 Conclusions

468 The withdrawal performance of STSs in bamboo scrimber has been investigated  
 469 experimentally and analytically. In the experimental programme, 210 specimens have been  
 470 tested to evaluate the effects of three key parameters on the withdrawal resistance of STSs,  
 471 namely the embedded length, the screw penetration angle and the self-tapping screw diameter.

472 The applicability of the calculation formulas for the withdrawal resistance of STSs in wood  
473 and original bamboo to STSs in bamboo scrimber has been examined. On this basis, a  
474 modified calculation formula for STSs in bamboo scrimber is proposed. From the results  
475 presented in the paper, the following conclusions may be drawn:

476 (1) Preliminary experimental results from STSs-bamboo scrimber specimens suggest a  
477 critical embedment slenderness ( $\lambda$ ) value of around 7.5; larger  $\lambda$  will lead to a failure mode  
478 with rupture of the STSs, while smaller  $\lambda$  tends to lead to STS pull-out failure. Furthermore,  
479 the material property test shows that the radial and tangential compressive strengths of  
480 bamboo scrimber are very close, therefore the bamboo scrimber may be generally assumed as  
481 a horizontally homogeneous material.

482 (2) Overall, the withdrawal resistance and rigidity of the STSs in the bamboo scrimber  
483 are similar to those of the STSs in wood. Both properties increase with the increase of the  
484 diameter of the STSs and the density of bamboo scrimber. Unlike the wood, however, the  
485 tensile strength and stiffness of STSs in the radial and tangential directions of the bamboo  
486 scrimber are very similar, so a unified calculation formula is recommended.

487 (3) From the test results, the 5<sup>th</sup> percentile value of the withdrawal resistance of STSs  
488 with  $\alpha=45^\circ$  appears to be close to or greater than that of STSs with  $\alpha=90^\circ$ . This observation is  
489 not in line with the trend in wooden structures. The specific relationship between the  
490 withdrawal resistance and the embedment angle in the bamboo scrimber requires further  
491 experimental evidences.

492 (4) Comparative analyses using different withdrawal resistance formulas suggest that the  
493 withdrawal capacity results of STSs calculated by the CCMC formula (Eq. 3) achieve better

494 accuracy. The CCMC (Eq. 3) formula is best suited as a basis for the calculation of the 5<sup>th</sup>  
495 percentile value of the withdrawal resistance of STSs in bamboo scrimber with  $\alpha=45^\circ$ .

496 (5) Based on the CCMC (Eq. 3) formula, a modified formula (Eq. 4) is proposed taking  
497 into account of the present experimental data. The proposed formula is further verified by the  
498 relevant test data from the literature, showing satisfactory accuracy. It should be noted that  
499 the applicability of the proposed formula for the withdrawal resistance of STSs in bamboo  
500 scrimber with other angles still requires further investigation.

## 501 **Acknowledgments**

502 This work was financially supported by the National Natural Science Foundation of China  
503 (51908291), the Nanjing Forestry University Youth Science and Technology Innovation Fund  
504 (CX2019002) and the Personal Scientific Research Start-up Funds (163020125, 163020657)  
505 from NFU.

## 506 **References**

- 507 [1] P. Van der Lugt, A. Van den Dobbelsteen, J. J. A. Janssen. , Constr. Build. Mater. 20 (9)  
508 (2006) 648-656.
- 509 [2] D. Yu, H. Tan, Y. Ruan. A future bamboo-structure residential building prototype in China:  
510 Life cycle assessment of energy use and carbon emission, Energ. Buildings. 43 (10) (2011) 2638-  
511 2646.
- 512 [3] Y. Xiao, R. Z. Yang, B. Shan. Production, environmental impact and mechanical properties of  
513 glubam, Constr. Build. Mater. 44 (2013) 765-73.
- 514 [4] B. Sharma, A. Gatóo, M. Bock, M. Ramage. Engineered bamboo for structural applications.

515 Constr. Build. Mater. 81 (2015) 66-73.

516 [5] M. Ahmad, F. A.Kamke. Properties of parallel strand lumber from Calcutta bamboo  
517 (*Dendrocalamus strictus*). Wood Sci Technol, 45(1) (2011) 63–72.

518 [6] P. Malanit, M. C.Barbu, A. Frühwald. Physical and mechanical properties of oriented strand  
519 lumber made from an Asian bamboo (*Dendrocalamus asper* Backer). Eur J Wood Wood Prod. 69(1)  
520 (2011) 27–36.

521 [7] D. Huang, Y. Bian, A. Zhou, B. Sheng. Experimental study on stress-strain relationships and  
522 failure mechanisms of parallel strand bamboo made from *phyllostachys*. Constr. Build. Mater. 77  
523 (2015) 130–138.

524 [8] H. Li, H. Zhang, Z. Qiu, J. Su, D. Wei, R Lorenzo, C. Yuan, H. Liu, C. Zhou. Mechanical  
525 properties and stress strain relationship models for bamboo scrimber. J Renew Mater. (2020) 13-  
526 27.

527 [9] P. Xie, W. Liu, Y. Hu, X. Meng, J. Huang. Size effect research of tensile strength of bamboo  
528 scrimber based on boundary effect model, Eng. Fract. Mech. 239 (2020) 107319.

529 [10] X. Sun, M. He, F. Liang, Z. Li, L. Wu, Y. Sun. Experimental investigation into the mechanical  
530 properties of scrimber composite for structural applications, Constr. Build. Mater. 276 (2021)  
531 122234.

532 [11] Y. Yu, R. Zhu, B. Wu, W. Yu. Fabrication, material properties, and application of bamboo  
533 scrimber, Wood Sci. Technol. 49 (1) (2015) 83-98.

534 [12] L. M. Tian, B. B. Jin, J. P. Hao. Research and application of modern bamboo structures,  
535 Engineering Mechanics. 5(36)(2019) 1-18.(in Chinese)

536 [13] Y. Xiao, Y. Wu, J. Li, R. Z. Yang. An experimental study on shear strength of glubam, Constr.

537 Build. Mater. 150 (2017) 490-500.

538 [14] Y. Huang, Y. Ji, W. Yu. Development of bamboo scrimber: a literature review, *J. Wood Sci.* 65  
539 (1) (2019) 1-0.

540 [15] G. Chen, Y.F. Yu, X. Li, B. He, Mechanical behavior of laminated bamboo lumber for  
541 structural application: an experimental investigation, *Eur. J. Wood Prod.* 78 (2020) 53–63,

542 [16] H. Li, B. J. Wang, L. Wang, P. Wei, Y. Wei, P. Wang. Characterizing engineering performance  
543 of bamboo-wood composite cross-laminated timber made from bamboo mat-curtain panel and  
544 hem-fir lumber, *Compos. Struct.* 266 (2021) 113785.

545 [17] B. Fei, R Liu, X. Liu, X. Chen, S. Zhang. A review of structure and characterization methods  
546 of bamboo pits. *Journal of Forestry Engineering*, 4(2) (2019) 13–18.

547 [18] C. Hong, H. Li, Z. Xiong, R. Lorenzo, I. Corbi, O. Corbi, D. Wei, C. Yuan, D. Yang, H.  
548 Zhang, Review of connections for engineered bamboo structures, *J. Build. Eng.* 30 (2020) 101324,

549 [19] B. Sharma, A. Gato, M. Bock, H. Mulligan, M. Ramage, Engineered bamboo: state of the art,  
550 *Constr Mater*, 168(2) (2014) 57-67.

551 [20] Y. Fu, H. Fang, F. Dai. Study on the properties of the recombinant bamboo by finite element  
552 method, *Compos. Part B-Eng.* 115 (2017) 151-159.

553 [21] X. Liu, X. Liu, J. Li. The test and analysis of nail holding power about recombinant bamboo  
554 used in furniture, *Wood processing machinery.* 28 (5) (2017) 10-12. (in Chinese)

555 [22] Y. Xiao, Q. Zhou, B. Shan. Design and construction of modern bamboo bridges, *J. Bridge*  
556 *Eng.* 15 (5) (2010) 533-541.

557 [23] H. Li, Z. Qiu, G. Wu, Li, O. Corbi, D. D. Wei, L. B. Wang, I. Corbi, and C. G. Yuan.  
558 Slenderness Ratio Effect on Eccentric Compression Properties of Parallel Bamboo Strand Lumber

559 Columns, *J. Struct. Eng.* 145 (8) (2019) 04019077.

560 [24] H. Li, G. Wu, Q. Zhang, A J Deeks, J Su. Ultimate bending capacity evaluation of laminated  
561 bamboo lumber beams, *Constr. Build. Mater.* 160 (2018) 365-375.

562 [25] Y. R. Shen, D. S. Huang, A. P. Zhou, D. Hui. An inelastic model for ultimate state analysis of  
563 CFRP reinforced PSB beams, *Compos. Part B-Eng.* 115(2017) 266-274.

564 [26] Y. Wei, S. Tang, X. Ji, K. Zhao, G. Li. Stress-strain behavior and model of bamboo scrimber  
565 under cyclic axial compression, *Eng. Struct.* 209 (2020) 110279.

566 [27] Z. Cui, M. Xu, Z. Chen, F. Wang. Experimental study on bearing capacity of bolted steel-  
567 PSB-steel connection. *Engineering Mechanics.* 36(1) (2019)96-103,118. (in Chinese)

568 [28] X. Li, Q. Mou, H. Ren, X. Li, Y. Zhong. Effects of moisture content and load orientation on  
569 dowel-bearing behavior of bamboo scrimber, *Constr. Build. Mater.* 262 (2020) 120864.

570 [29] G. Chen, W. Yang, T. Zhou, Y. Yu, J. Wu, H. Jiang, et al. Experiments on laminated bamboo  
571 lumber nailed connections. *Constr Build Mater.* 269 (2021) 121321.

572 [30] R. Tomasi, A. Crosatti, M. Piazza. Theoretical and experimental analysis of timber-to-timber  
573 joints connected with inclined screws, *Constr. Build. Mater.* 24(9) (2010) 1560-1571.

574 [31] L. Righetti, M. Corradi, A. Borri. Shear resistance of screwed timber connections with  
575 parallel to grain FRP reinforcements, *The14th World Conference on Timber Engineering*  
576 *(WCTE2016)*, 2016.

577 [32] H. M. Li, F. Lam, H. Qiu. Flexural performance of spliced beam connected and reinforced  
578 with self-tapping wood screws, *Eng. Struct.* 152 (2017) 523-34.

579 [33] H. M. Li, F. Lam, H. Qiu. Comparison of glulam beam-to-beam connections with round  
580 dovetail and half-lap joints reinforced with self-tapping screws, *Constr. Build. Mater.* 227 (2019)



581 116437.

582 [34] T. Tannert, F. Lam. Self-tapping screws as reinforcement for rounded dovetail connections,  
583 Struct. Control Hlth. 16 (3) (2009) 374-384.

584 [35] A. Hossain, D. Ilana, T. Tannert. Cross-Laminated Timber Shear Connections with Double-  
585 Angled Self-Tapping Screw Assemblies. J. Struct. Eng. 142(11) (2016) 04016099.

586 [36] S.Y. Huang, A Study on the Design of New-Sino-Style Furniture Made of Recombinant  
587 Bamboo, Nanjing Forestry University, Nanjing, China, 2011.

588 [37] Y. Chen, S. Zhu, Y. Guo, S. Liu, D. Tu, H. Fan. Investigation on withdrawal resistance of  
589 screws in reconstituted bamboo lumber. Wood Research, 61 (5) (2016) 799-810.

590 [38] K. A. Harries, Morrill P, Gauss C, et al. Screw withdrawal capacity of full-culm *P. edulis*  
591 bamboo, Constr. Build. Mater. 216 (2019) 531-541.

592 [39] J.Q. Li, L.H. Chen, T. Su, Study on bolt joint intensity of laminated bamboo for furniture,  
593 J.Fujian.Fujian.For 31 (3) (2011) 271–275.

594 [40] H.W. Zhang, Study on the Optimize Design for Parameters of Screw Thread Used in Glued  
595 Laminated Bamboo and the Mechanical Property, Nanjing Forestry University, Nanjing, China,  
596 2012.

597 [41] BS EN 1995-1-1, Eurocode 5: Design of timber structures-Part 1-1: General-common rules  
598 and rules for buildings. London: British Standards Institution, 2004

599 [42] CCMC. Evaluation report CCMC 13677-R SWG ASSY and VG plus and SWG ASSY 3.0  
600 self-tapping wood screws. Canadian Construction Material Center, Ottawa, 2013

601 [43] Trujillo D J A, Malkowska D. Empirically derived connection design properties for Guadua  
602 bamboo, Constr. Build. Mater. 2018, 163: 9-20.

603 [44] JG/T 199-2007. Testing methods for physical and mechanical properties of bamboo used in  
604 building. Beijing, China: China Standard Press, 2007 (in Chinese).

605 [45] GB/T1935-2009 Method of testing in compressive strength parallel to grain of wood (in  
606 Chinese).

607 [46] GB/T 1939-2009 Method of testing in compressive strength perpendicular to grain of wood.  
608 (in Chinese).

609 [47] GB/T 1936.2-2009. Method for determination of the modulus of elasticity in static bending  
610 of Wood. Chinese national standard. China Standard Press, 2009 (in Chinese).

611 [48] D. Huang, Y. Bian, A. Zhou, B. Sheng. Experimental study on stress–strain relationships and  
612 failure mechanisms of parallel strand bamboo made from phyllostachys. *Constr Build Mater.* 77  
613 (2015) 130-8.

614 [49] Lv H. The renovation and demonstration of the traditional rural dwellings construction  
615 technology. Beijing: China architecture and building press, 2018.09:60-62. (in Chinese).

616 [50] ASTM D1761 Standard test methods for mechanical fasteners in wood. Philadelphia, PA,  
617 2006.

618 [51] LY/T 2377-2014, Test methods for the joint performance with dowel type fasteners used in  
619 wooden structural material. 2012 (in Chinese).

620 [52] CAN, CSA-O86.09. Engineering design in wood (limit states design). Canadian Standards  
621 Association (CSA), Mississauga, 2014.

622 [53] ASTM D5652 Standard test methods for bolted connections in wood and wood-base.

623 [54]Barrett J D, Jones E D, Lau W. Canadian lumber properties. Ottawa: Canadian Wood Council,  
624 1994.

625 [55] Canadian Wood Council (CWC). Wood design manual. Ottawa:2015.

626